Resting state functional connectivity in the human spinal cord at 7 Tesla

Robert L Barry[1,2], Seth A Smith[1,2], and John C Gore[1,2]

[1]*Vanderbilt University Institute of Imaging Science, Nashville, TN, United States,* [2]*Department of Radiology and Radiological Sciences, Vanderbilt University Medical Center, Nashville, TN, United States*

Introduction

The field of functional magnetic resonance imaging (fMRI) has rapidly expanded since its emergence two decades ago [1-4], and fMRI using blood oxygenation level dependent (BOLD) contrast is the most commonly used method for detecting signal changes *in vivo*. In 1995, Biswal et al. [5] established the existence of low-frequency correlations between BOLD signal fluctuations in the brain when no task was performed (i.e., the resting state). The identification of patterns of highly correlated low-frequency MR signals in the resting brain provides a powerful approach to delineate and describe neural circuits, and an unprecedented ability to assess the manner in which distributed regions work together to achieve specific functions. Thousands of fMRI studies have provided a wealth of knowledge about the functional architecture of the brain, and to date over 3000 published resting state studies establish the widespread utility of these methods to non-invasively detect and characterize low-frequency functional connectivity across multiple cortical areas. However, nearly all of these studies explored only the brain, and there have been very few investigations of spinal cord function. fMRI in the spinal cord was first demonstrated by Yoshizawa et al. [6] in 1996, and task-based (motor and/or sensory) spinal fMRI has since been demonstrated by a handful of groups worldwide (e.g., [7-14]). To date only one study has attempted to investigate resting state BOLD fluctuations in the human spinal cord [15], and was performed at low field (1.5 T) with low spatial resolution and spatial smoothing [15]. The advent of 7 T scanners and implementation of multichannel spine array coils along with appropriate image acquisitions and corrections provide new opportunities for high-resolution fMRI of the spinal cord with high sensitivity to BOLD fluctuations in the small gray matter structures that are typically not well visualized in BOLD fMRI scans of the cord. The goal of this research is to exploit our newly developed methods for human spinal fMRI at 7 T to perform high-resolution ultra-high-field investigation of low-frequency functional connectivity in the human cervical spinal cord.

Methods

Experiments were performed on a Philips Achieva 7 T scanner with a custom-designed 16-channel coil for 7 T spinal imaging (Nova Medical Inc.). Healthy volunteers were scanned under a protocol approved by the institutional review board. fMRI data were acquired with a 3D fast field echo [16,17] sequence designed to minimize T_2^* blurring and geometric distortions. Twelve 4-mm slices covering vertebrae C3 to C5 were acquired with 0.91 x 0.91 x 4 mm^3 voxels every 3.49 seconds (291 ms/slice). One hundred resting state volumes were acquired. Data were corrected for physiological noise using RETROICOR [18] and slice-specific 'regressors of no interest' (constructed via principal component analysis on all cerebrospinal fluid voxels). Functional data were warped to the anatomcial and resampled (with sinc interpolation) to 0.31 x 0.31 x 4 mm^3 voxels. A gray matter mask was manually delineated from each anatomic slice (Fig. 1A) and applied to all co-registered functional images. Mean/median temporal signal-to-noise ratio (TSNR) = 30 across spinal gray matter with the highest TSNR (up to 50) observed in the ventral horns.

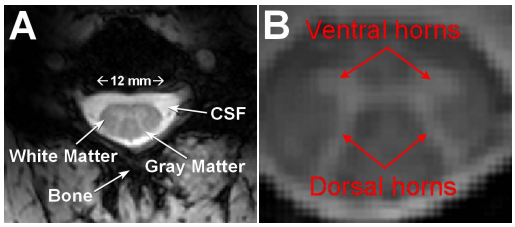

FIG. 1: Anatomy of the human cervical spinal cord. (**A**) High-resolution T_2^*-weighted axial image. Excellent conspicuity permits visualization of the characteristic butterfly-shaped gray matter column. (**B**) Left and right dorsal horns contain sensory neurons and left and right ventral horns contain motor neurons.

Hypothesis of functional connectivity: Given the known anatomical connections within the spinal cord (see Figs. 4-9 and 36-2A in [19]) and the existence of central pattern generators throughout mammalian spinal cords [19-22], we hypothesized that we should observe low-frequency BOLD correlations between dorsal horn and ipsilateral ventral horn and between dorsal/ventral horns and contralateral dorsal/ventral horns within an axial slice (Fig. 1B). We further hypothesized that we should observe functional connectivity within ipsilateral dorsal and ventral horns along the cord. Resting state data were band-pass filtered between 0.01 Hz and 0.08 Hz using a Chebyshev Type II filter in Matlab (`cheby2`) to emphasize low-frequency signals of interest. The linear correlation coefficient (r) was calculated between a seed voxel and all other voxels. These correlation values were converted to z-scores using the Fisher r-to-z transformation $z = \tanh^{-1}(r)(dof-3)^{1/2}$ where dof is the estimated degrees of freedom for each voxel after correction for the first-order autocorrelation [23].

Results

Figure 2 presents a functional connectivity analysis of a single resting state run from a healthy 40-year-old male. The median dof correction factor was 0.55 (min = 0.26; max = 0.82), revealing that the actual degrees of freedom were about half the number of time points; not performing this correction would have significantly (and artificially) inflated z-scores. The seed selected was a single gray matter voxel with high TSNR (= 50) in the center of the left ventral horn in C3. Within-slice correlations are observed between this seed and ipsilateral dorsal horn and contralateral ventral and dorsal horns. Significant positive correlations are also observed in ventral horns on adjacent slices, and across ventral and dorsal horns on all four slices in C4. Interestingly, regions of significant negative correlations are also observed in ventral and dorsal horns on both adjacent slices and three of four slices in C5.

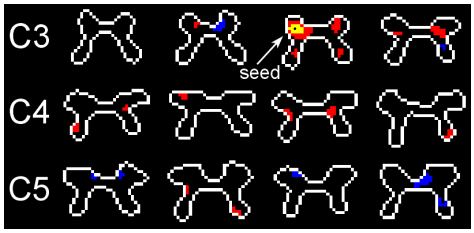

FIG. 2: Functional connectivity analysis in spinal gray matter of a control subject. A threshold of $|z| > 2$ corresponds to an approximate 95% confidence interval. A minimum cluster threshold of three contiguous voxels protects against spurious correlations. [Color legend: yellow is $z > 5$, red is $2 < z \leq 5$, and blue is $z < -2$.]

Discussion

We believe that this abstract represents the first demonstration of high-resolution resting state functional connectivity in the human spinal cord. The use of an ultra-high field scanner with a novel 16-channel spine receive coil facilitates the acquisition of T_2^*-weighted images with sub-millimeter in-plane resolution and high sensitivity to BOLD fluctuations [24]. The results presented in Fig. 2 support the hypothesis of functional connectivity between the seed voxel and ipsilateral dorsal horn ($z = 2.7$), contralateral ventral horn ($z = 2.7$), and contralateral dorsal horn ($z = 2.9$). Furthermore, regions of significant correlation on adjacent slices ($z_{max} = 3.3$) and other slices ($z_{max} = 3.0$) further support the hypothesis of functional connectivity along the spinal cord. The apparent absence of connectivity in the horns on some slices may be due to regions of lower TSNR and unavoidable through-plane partial volume effects due to increasing cross-sectional area of the gray matter butterfly in inferior slices. Our ongoing work includes continual refinement of the functional protocol, quantification of within- and between-subject reproducibility of spinal functional connectivity, and further investigation of the reproducibility of regions of negative temporal correlations. Future work will investigate modulation of resting state spinal functional connectivity in cohorts of patients with multiple sclerosis and spinal cord injury, and attempt to translate these methods down to 3 T to facilitate widespread development of clinical applications.

Acknowledgments – This research was supported by NIH grants 5R01EB000461 and 5K01EB009120.

References – [**1**] Ogawa et al. PNAS USA 1990;87:9868. [**2**] Kwong et al. PNAS USA 1992;89:5675. [**3**] Ogawa et al. PNAS USA 1992;89:5951. [**4**] Bandettini et al. MRM 1992;25:390. [**5**] Biswal et al. MRM 1995;34:537. [**6**] Yoshizawa et al. Neuroimage 1996;4:174. [**7**] Stroman et al. MRM 1999;42:571. [**8**] Madi et al. AJNR 2001;22:1768. [**9**] Backes et al. AJNR 2001;22:1854. [**10**] Moffitt et al. JMRI 2005; 21:527. [**11**] Maieron et al. J Neurosci 2007;27:4182. [**12**] Agosta et al. HBM 2009;30:340. [**13**] Cohen-Adad et al. Neuroimage 2010;50:1074. [**14**] Brooks et al. J Neurosci 2012;32:6231. [**15**] Wei et al. Eur J Appl Physiol 2010;108:265. [**16**] van der Meulen et al. MRI 1988;6:355. [**17**] Barry et al. Neuroimage 2011;55:1034. [**18**] Glover et al. MRM 2000;44:162. [**19**] Kandel et al. 'Principles of neural science, 4th ed., 2000. [**20**] Viala & Freton. Exp Brain Res 1983;49:247. [**21**] Gordon et al. J Neurophysiol 2008;100:117. [**22**] Juvin et al. J Neurosci 2012;32:953. [**23**] Rogers & Gore. PLoS ONE 2008;3:e3708. [**24**] Ogawa et al. Biophys J 1993;64:803.